Optimization of Crank Angles to Reduce Excitation Forces and Moments in Engines

Jeong-Geun Park
Enging & Plant Technology Division, Stx Engine Co., 80, Seongsan-Dong, Changwon, Gyeongsangnam-Do, 641-315, Korea
Weui-Bong Jeong
School of Mechanical Engineering, Pusan National University, San 30, Jangjeon-Dong, Geumjeong-Gu, Busan 609-735, Korea
Young-Soo Seo
Naval Systems Development Center, Agency for Defence Development, P.O.Box 18, Chinhae, Gyeongsangnam-Do, 645-600, Korea
Wan-Suk Yoo*
School of Mechanical Engineering, Pusan National University, San 30, Jangjeon-Dong, Geumjeong-Gu, Busan 609-735, Korea

The forces from the engine firings and the rotational motion of a crankshaft cause excitations in vehicle engines. In conventional in-line engines, crank angles might be evenly assigned by dividing 360 degrees by the number of cylinders. In this paper, allocation of crank angles was carried out in two different ways, (1) to minimize the moments excited in an engine and (2) to minimize the forces transmitted to the engine mounts. The forces and moments due to gas pressure and reciprocating parts in the engine were formulated, and a computer program to predict the excitation forces and moments was developed. The developed program was applied to a four-stroke seven-cylinder engine to reduce the first- and the second- order moments produced by the engine. Then, it was also applied to minimize the forces transmitted to the engine mounts. The optimized crank angles, in contrast to those of conventional engines, were not evenly distributed. The moments and forces were reduced with the optimized crank angles.

Key Words : Optimal Design, Crank angles, Engine Excitation Forces, The First Order Moment, The Second Order Moment

1. Introduction

The two main sources of engine excitations are variation of gas pressure in a cylinder and fluctuating forces from reciprocating parts. These excitations are transmitted to the body and thus result in structure-borne vibrations and noises. One of the active ways to reduce these vibrations and noises is to reduce engine excitations by assigning crank angles properly or to reduce the masses of the reciprocating parts. A passive way is to design engine mounts that reduce transmitted forces.

As stated, a passive way to reduce these vibrations is usage of specially designed engine mounts. An optimization technique has also been applied to minimize the transmission of engine vibration (Pasricha, 1979). The optimum values of a marine engine mount have been selected to reduce the transmissibility of engine vibration to the

* Corresponding Author,
E-mail : wsyoo@pusan.ac.kr
TEL : +82-51-510-2328; **FAX** : +82-51-581-8514
School of Mechanical Engineering, Pusan National University, San 30, Jangjeon-Dong, Geumjeong-Gu, Busan 609-735, Korea. (Manuscript **Received** September 6, 2006; **Revised** December 8, 2006)

chassis (Snyman, 1995).

A fluid-structure interaction FEA (finite element analysis) and nonlinear FEA technology have been used to estimate system parameters (Shangguan, 2004).

It has also been reported that the cyclic variation of the polar moments of inertia of reciprocating parts causes a periodic variation of frequencies and amplitudes in reciprocating engine systems. Large variations in inertial torques invokes secondary resonance in the torsional vibration of marine diesel engines (Paricha, 1976).

To reduce the excitations from gas pressure, forces from gas pressure variation should be included in analysis, and the motion of the slider crank also should be derived as a function of gas pressure (Denman, 1991). For a precise investigation of gas pressure, a model relating cylinder combustion pressure to the angular velocity of the crankshaft has been presented (Connolly, 1994). As a result, the governing nonlinear differential equation for the pressure process is converted to a linear differential equation by changing the independent variable from time to crank angles.

Another active strategy to reduce these vibrations is to minimize the noise and vibration in the engine itself. The optimization technique has been directly applied to reduce the noise and vibration optimization of an eleven-cylinder marine engine (Jacobsen, 1995). The target function was chosen to minimize the external first- and second-order moments. To analyze and optimize these moments, a fundamental derivation of the engine excitation forces and moments was derived. The firing order of a four-stroke nine-cylinder marine engine was studied (Ronnedal, 2003). Among 430,320 possible firing order combinations, 28 combinations were chosen to preserve the first- and the second-order moments within the prescribed value. In that research, the crank angle allocation was not included.

In addition to engine optimization, there had been researches for the optimization of crankshaft. Dubensky (2002) reviewed the process design of the crankshaft and proposed an evolving flow chart of tasks at the concept stage of crankshaft design. Kim (2003) treated a small compressor used for refrigerator to determine the coupled dynamic behavior of the piston and the crankshaft. Suh (2003) proposed a simplified model of the crankshaft in the large marine engine, and Cho (1995) studied an optimization of the crankshaft in a in-line 6-cylinder diesel engine.

In the present study, crank angles were first optimized to reduce the maximum values of the first- and the second-order moments. Then, the crank angles were also optimized to minimize the forces transmitted to the engine moments. With the optimized crank angles, which were not evenly distributed, the engine moments were much reduced. As described in Section 2, the exerted forces and moments of a single cylinder were derived, and in Section 3, the total exertion force on the engine is explained. In Section 4, the optimization process is explained as well as the optimized result minimizing the excitation moments. In Section 5, the optimized results minimizing the forces transmitted to the engine mounts are explained, in Section 6, conclusions are provided.

2. Forces and Moments in a Single Cylinder

2.1 Forces in translational and rotational directions

Figure 1 shows a slider crank mechanism and the direction of the coordinates in one cylinder. When the mass of the crank m_{crk} and the mass of the connecting rod m_{con} are assumed to be

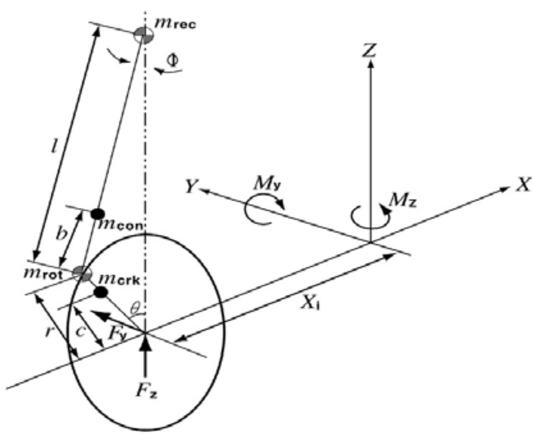

Fig. 1 Applied forces and moments at an engine

concentrated at the center of mass, the reciprocating mass m_{rec} and the rotating mass m_{rot} of the mechanism can be written as

$$m_{rec}=m_p+\left(\frac{b}{l}\right)m_{con} \tag{1}$$

$$m_{rot}=\left(\frac{c}{r}\right)m_{crk}+\left(1-\frac{b}{l}\right)m_{con} \tag{2}$$

where m_p is the mass of the piston, b and c are the distances from the joints to the centers of mass of the crank and the connecting rod, respectively, as shown in Fig. 1.

The reaction forces of one cylinder are shown in Fig. 2. The vertical force P is combined with the piston force from combustion and the force from the reciprocating part. This force P is resolved into the force S in the connecting rod and into the force G in the horizontal direction. The transmitted force S exerts two forces on the crank, the radial force R and the tangential force T, respectively. The distance h in Fig. 2 can be written as

$$h=r\left(\cos\theta+\frac{l}{r}\cos\phi\right) \tag{3}$$

where r and l are the radius of the crank and the length of the connecting rod, respectively. And θ is the angle between the crank and the vertical axis, while ϕ is the angle between the connecting rod and the vertical line. Defining $\lambda=r/l$ and expanding the above equation with a Taylor series, the distance can be rewritten as

$$h=r\left(\begin{array}{c}\cos\theta+a_0+a_2\cos 2\theta\\+a_4\cos 4\theta+a_6\cos 6\theta+\cdots\end{array}\right) \tag{4}$$

where $a_0, a_2, a_4, \cdots$ are the following coefficients:

$$a_0=\frac{1}{\gamma}\left[1-\left(\frac{1}{4}\lambda^2+\frac{3}{64}\lambda^4+\frac{5}{256}\lambda^6+\cdots\right)\right] \tag{5}$$

$$a_2=\frac{l}{\gamma}\left[\frac{1}{4}\lambda^2+\frac{1}{16}\lambda^4+\frac{15}{512}\lambda^6+\cdots\right] \tag{6}$$

$$a_4=-\frac{l}{r}\left[\frac{1}{64}\lambda^4+\frac{3}{256}\lambda^6+\cdots\right] \tag{7}$$

$$a_6=\frac{l}{r}\left[\frac{1}{512}\lambda^6+\cdots\right] \tag{8}$$

The reciprocating inertial force can be derived as

$$\begin{aligned}\vec{F}_{rec}&=m_{rec}\ddot{h}\\&=r\omega^2 m_{rec}\left(\begin{array}{c}\cos\theta+4a_2\cos 2\theta\\+16a_4\cos 4\theta\\+36a_6\cos 6\theta+\cdots\end{array}\right)\vec{e}_z\end{aligned} \tag{9}$$

The rotational inertial forces are combined with the rotational mass component and the counter mass component as

$$\begin{aligned}\vec{F}_{rot}&=(F_{rot,z}+F_{cw,z})\,\vec{e}_z+(F_{rot,y}+F_{cw,y})\,\vec{e}_y\\&=[m_{rot}r\omega^2\sin\theta+m_{cw}r_{cw}\omega^2\sin(\theta+\psi)]\,\vec{e}_y\\&\quad+[m_{rot}r\omega^2\cos\theta+m_{cw}r_{cw}\omega^2\cos(\theta+\psi)]\,\vec{e}_z\end{aligned} \tag{10}$$

where m_{cw} and r_{cw} represent the counter mass and the distance from the rotational center to the counter mass, respectively. The angle ψ is the angle between the crank and the counter weight.

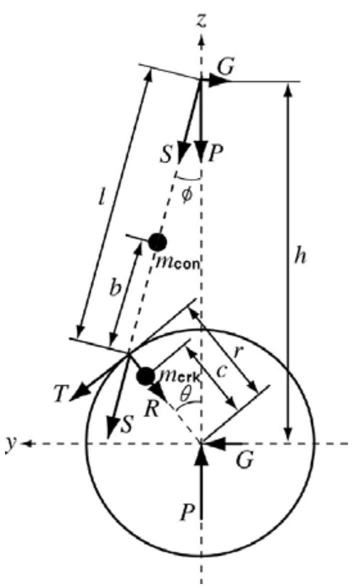

Fig. 2 Applied forces at a cylinder

2.2 Gas force, guide force, and guide moment

The vertical force due to combustion depends on the gas pressure in the cylinder. Fig. 3 shows a typical gas pressure of a four-stroke engine, which completes one cycle in two revolutions. The pressure is measured from 0°, which states the position of TDC (top dead center). Then,

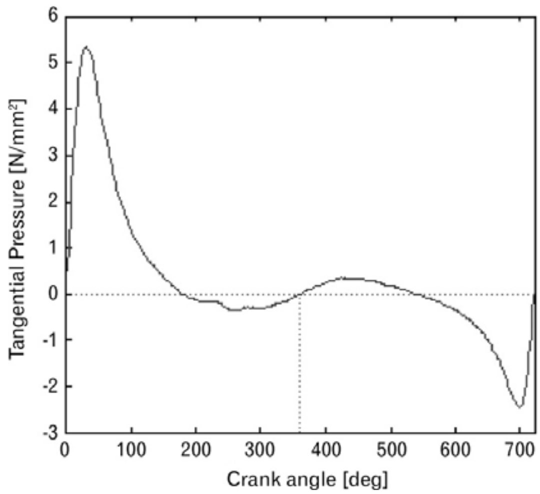

Fig. 3 Gas pressure in a cylinder

the gas forces can be written as

$$\vec{F}_{gas}=F_{gas}\vec{e}_z = \frac{\pi d^2}{4}\sum_k (c_k \cos k\theta + d_k \sin k\theta)\,\vec{e}_z \tag{11}$$

where c_k and d_k are Fourier constants representing the gas pressure shown in Fig. 3, and k are 0.5, 1.0, 1.5, $\cdots$ for four stroke engines.

Due to the y-directional component of the force in the connecting rod, the guide force G shown in Fig. 2 can be calculated as

$$\begin{aligned}\vec{F}_{guide}&=\vec{G}\\ &=\vec{P}\tan\phi\\ &=(F_{gas}+F_{rec})\tan\phi\,\vec{e}_y\\ &=(F_{gas}+F_{rec})\frac{\lambda\sin\theta}{\sqrt{1-\lambda^2\sin^2\theta}}\vec{e}_y\end{aligned} \tag{12}$$

where the force P is the vertical force, as shown in Fig. 2.

Since the same magnitude of force is acting on the rotational center of the crank, the summation of this guide force is zero. But it generates the guide moment about the rotational center of the crank as

$$\begin{aligned}\vec{M}_{guide}&=\vec{h}\times\vec{G}\\ &=\vec{h}\times\vec{S}\sin\phi\\ &=\vec{r}\times\vec{T}\\ &=r\cdot S\sin(\theta+\phi)\,\vec{e}_x\end{aligned} \tag{13}$$

3. Forces and Moments in an Engine

3.1 Total forces produced by a cylinder

The forces produced by a cylinder are transferred to the engine with three directional forces and moments. The translational forces can be easily represented by adding all force terms as

$$\vec{F}_i=\begin{bmatrix}F_x\\F_y\\F_z\end{bmatrix}_i=\begin{bmatrix}0\\(\vec{F}_{rot})_{,y}\\(\vec{F}_{rec}+\vec{F}_{rot})_{,z}\end{bmatrix}_i \tag{14}$$

where the summation of the guide force is zero.

The moments produced by the ith cylinder forces can be determined by the cross products of the distance vectors and force vectors as

$$\vec{M}_i=\begin{bmatrix}M_x\\M_y\\M_z\end{bmatrix} =\begin{pmatrix}\vec{r}_{i,rec}\times\vec{F}_{i,rec}+\vec{r}_{i,rot}\times\vec{F}_{i,rot}\\ +\vec{r}_{i,cw}\times\vec{F}_{i,cw}+\vec{M}_{i,guide}\end{pmatrix} \tag{15}$$

where $\vec{r}_{i,rec}$, $\vec{r}_{i,rot}$, and $\vec{r}_{i,cw}$ are the vectors from the centers of the reciprocating part, the rotating part, the counter weight, respectively.

$$\vec{r}_{i,rec}=\begin{bmatrix}x_i\\y_i\\z_i+r\cos(\theta_i+\phi_i)+l\sqrt{1-(\lambda\sin(\theta_i+\phi_i))^2}\end{bmatrix} \tag{16}$$

$$\vec{r}_{i,rot}=\begin{bmatrix}x_i\\y_i+r\sin\theta_i\\z_i+r\cos\theta_i\end{bmatrix} \tag{17}$$

$$\vec{r}_{i,cw}=\begin{bmatrix}x_i\\y_i+r_{cw}\sin(\theta_i+\psi_i)\\z_i+r_{cw}\sin(\theta_i+\psi_i)\end{bmatrix} \tag{18}$$

The total forces and moments from a multi-cylinder engine can be obtained by summing all the components.

$$\begin{aligned}\vec{F}&=\sum_{i=1}\vec{F}_i\\ \vec{M}&=\sum_{i=1}\vec{M}_i\end{aligned} \tag{19}$$

Figure 4 shows the configuration of an in-line engine and the associatedmoments. As shown in the Fig., the rotational force $\vec{F}_{rot}$ acting on the centerline of the crankshaft generates forces and the first-order moment.

The reciprocating force $\vec{F}_{rec}$ exerts the first-order moment and the second-order moment. The guide force $\vec{F}_{guide}$ exerts the H-type guide moment, which is also shown in Fig. 4. For the H-type guide moment, the directions of the forces at the guide plane and the forces at the crankshaft are opposite directions at each plane.

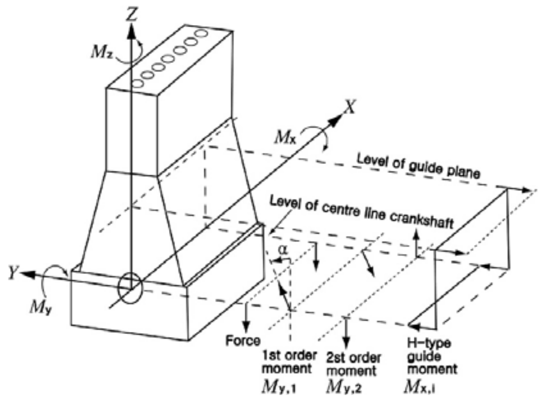

Fig. 4 Forces and moments at a multi-cylinder engine

Table 1 Specifications of an engine used for the force calculation

rpm	750 [rpm]
firing order	1-6-3-4-5-2-7
crank radius, r	0.16 [m]
con.rod length, l	0.64 [m]
con.rod mass, m_{con}	93.657 [kg]
con.rod mass eccentric length, b	0.2051 [m]
crank throw mass, m_{crk}	227.19 [kg]
crank throw eccentric length, c	0.0802 [m]
Piston diameter	0.28 [m]
piston mass	60.452 [kg]
counterweight mass	181.478 [kg]
counterweight length	0.1831 [m]
counterweight phase	180°
crank position, (x_i, y_i, z_i)	(1.44,0,0), (0.96,0,0), (0.48,0,0), (0,0,0), (−0.48,0,0), (−0.96,0,0), (−1.44,0,0)

3.2 Calculation of forces and moments

To evaluate the derived forces and moments for the engine, a typical seven- cylinder engine was selected. The specifications of the selected engine are shown in Table 1.

From the derived equations for the forces and moments, the excitation moments are calculated from the derived formula. The sum of vertical moment $M_{y,1}+M_{y,2}$, and the horizontal moment M_z shown in Fig. 5, are compared with the manufactures' specifications in Table 2. Since the engine speed was assigned to 750 rpm, the first-order frequency in Table 2 is 12.5 Hz.

As shown in Table 2, two values are very close. Thus, the developed computer program to calcu-

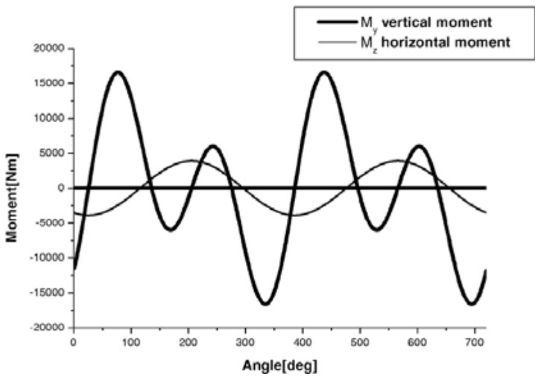

Fig. 5 Excitation moments at an engine calculated by the derived formula

Table 2 Comparison of calculated moments versus manufacturer's specifications

Order	Moments	Freq. [Hz]	Magnitude [kNm]	
			Estimated value	Manufactures' spec.
1.0	M_z	12.5	3.89	3.8
1.0	$M_{y,1}$	12.5	7.56	7.6
2.0	$M_{y,2}$	25.0	10.95	11
3.5	$(M_{x,i})_{,1}$	43.75	27.96	28.7
7.0	$(M_{x,i})_{,2}$	87.5	4.82	4.4
(∗) All Forces [kN]			0.0	0.0

late the forces and moments was validated.

4. Optimal Crank Angles to Minimize Moments

Since the forces and moments exerted on an engine due to the reciprocating part and gas pressure exert high-order excitation forces, these forces and moments must be reduced. As described in Section 4 and Section 5 employing the optimization process, the crank angles were relocated to reduce these exerting forces and moments on a seven-cylinder engine.

4.1 Objective function, design variables, and constraints

For the optimization, the following objective function was chosen to minimize the exerted moments on the engine, preserving the summation of exerting forces as zero.

$$J=\sqrt{\left(\sum_{i=1}^{p} M_{x,i}^2\right)+M_{y,1}^2+M_{y,2}^2+M_z^2} \tag{20}$$

where p is the order selected by the designer. And the $M_{x,i}, M_{y,1}, M_{y,2}$, and M_z are the ith-order guide moment, the first-order and the second-order moments in the vertical direction, and the horizontal moment, respectively, as shown in Fig. 4.

The design variables were selected according to the crank angles of the seven cylinders. To preserve the non-equivalent forces acting on the engine as zero, the following constraints were selected :

$$\begin{gathered}\sum_{i=1}^{7}\sin\theta_i=0,\ \sum_{i=1}^{7}\cos\theta_i=0,\\ \sum_{i=1}^{7}\sin 2\theta_i=0,\ \text{and}\ \sum_{i=1}^{7}\cos 2\theta_i=0\end{gathered} \tag{21}$$

4.2 Optimization process

When the crank angle for the first cylinder was assigned as zero, the design variables for the seven-cylinder engine became six. Since there were the four equality constraint equations of (21) between these six design variables, the independent variables were just two. If the first angle θ_1 is set to zero, the second angle θ_2 and the third angle θ_3 are assigned as independent design variables ; then, the other four angles $\theta_4, \theta_5, \theta_6$, and θ_7 can be determined by nonlinear constraint equations, which can be solved with the Newton-Raphson nonlinear equation solver (Paricha and Carnegie, 1976).

Since the dependent design variables $\theta_4, \theta_5, \theta_6$, and θ_7 could be calculated from the independent design variables θ_2 and θ_3, the optimization process could be changed to an optimization without constraint equations. For this unconstrained minimization problem, the steepest decent method, with golden section search, was employed (Paricha and Carnegie, 1979).

The following process was used for the unconstrained minimization technique.

Step 1 : Define the objective function, assign the convergence parameter, and calculate the first order derivatives.

Objective function

$$J=\sqrt{\left(\sum_{i=1}^{p} M_{x,i}^2\right)+M_{y,1}^2+M_{y,2}^2+M_z^2}$$

and the first-order derivatives $\partial J/\partial\theta_2$ and $\partial J/\partial\theta_3$. The convergence parameter ε may be assigned by the designer ; the value of 0.01 was used in this research.

Step 2 : Initialize the design variables and assign the iteration count $k=0$. Input the initial values of the design variable θ_i, $i=1,2,\cdots,7$. The initial guess for the design variables may be assigned by Equal distribution.

Step 3 : Start iteration to find new values for θ_2 and θ_3. Using the derivatives, find the new values of θ_2 and θ_3 by the search technique

$$\begin{pmatrix}\theta_2^{k+1}\\ \theta_3^{k+1}\end{pmatrix}=\begin{pmatrix}\theta_2^{k}\\ \theta_3^{k}\end{pmatrix}-\alpha_k\begin{bmatrix}\partial J/\partial\theta_2\\ \partial J/\partial\theta_3\end{bmatrix}^k$$

where the step size α_k is determined by golden section search (Paricha and Carnegie, 1979). When the increments in variables are smaller than the criterion, stop. Otherwise, repeat the iteration until the prescribed criterion is satisfied. When the new variables θ_2 and θ_3 are obtained, then calculate

Table 3 Initial and optimized crank angles minimizing exerted moments

Cylinder No.	initial crank angle	optimized crank angle
1	0.0°	0.0°
2	257.1°	258.5°
3	102.9°	103.9°
4	154.3°	158.4°
5	205.7°	209.5°
6	51.4°	57.6°
7	308.6°	314.6°

Table 4 Moments on the engine

Order	Moments	Freq. [Hz]	Amplitude[kNm]	
			before optimized	after optimized
1.0	M_z	12.5	3.89	1.1
1.0	$M_{x,1}$	12.5	0.5E-3	2.68E-2
1.0	$M_{y,1}$	12.5	7.56	2.1
2.0	$M_{y,2}$	25.0	10.95	9.94
3.5	$M_{x,1}$	43.75	27.96	27.7
7.0	$M_{x,2}$	87.5	4.82	4.63

the dependent design variables $\theta_4, \theta_5, \cdots, \theta_7$.

4.3 Results from moments optimization

Table 3 shows the optimized crank angles, calculated in this research, which show changes from the initial values. Although the initial values are evenly distributed, the optimized values are unevenly allocated. In Table 4, the moments before and after the optimization are shown. With the optimized values, the maximum reduction was 72% in the vertical moment, but there were almost no changes in the guide moments. The reason was that the guide moment came mainly from the gas forces, which could not be reduced by the crank angles.

Figures 6~8 show the moment variations according to the crank angles. The total vertical moment M_y in Fig. 6 and the horizontal moment M_z in Fig. 7 are much reduced. But the amplitude in the guide moment $M_{x,1}$ in Fig. 8, which is also shown in Table 4, shows almost no changes.

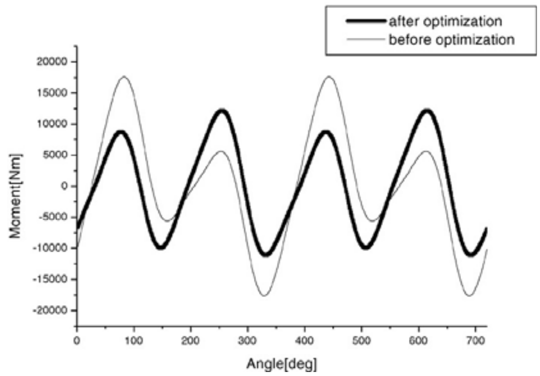

Fig. 6 Comparison of the total vertical moment $M_{y,1}+M_{y,2}$

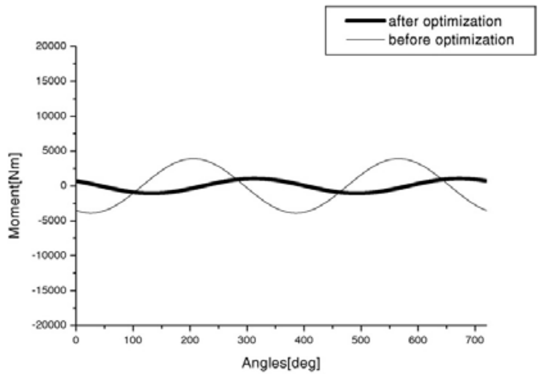

Fig. 7 Comparison of the horizontal moment M_z

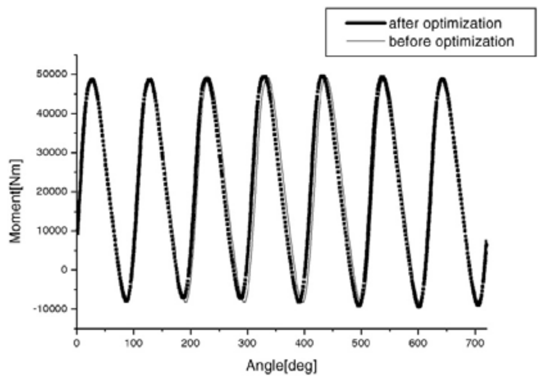

Fig. 8 Comparison of the guide moment $M_{x,1}$

5. Optimal Crank Angles to Minimize Transmitted Forces

The moments and forces generated by an engine exert vibrations in a vehicle chassis or marine hull. Reducing these forces transmitted through mounts is also required to reduce the vibration of the vehicle chassis or the marine hull. As described in this section, the optimization program discussed in Section 4 was also applied to the optimal design of crank angles to minimize the transmitted forces. The same engine as shown in Table 1 was used, and a schematic diagram of the engine-mount system is shown in Fig. 9. The positions of the mounts with respect to the mass center of the engine are given in Table 5. The stiffness values of four equivalent engine mounts were obtained from the manufacturer's company as k_z=4,850 kN/m in the longitudinal direction and $k_x=k_y$=600 kN/m in the transverse direction.

Assuming the engine to be rigid, the motion of the engine with six degrees of freedom can be calculated from the exerted moments and forces. The forces transmitted through the mounts can also be calculated from the behavior of the engine. Fig. 10 shows the forces transmitted through mount k_1 when crank angles are evenly distributed. The magnitudes of the forces transmitted through engine mounts k_2, k_3, and k_4 were similar to that of mount k_1.

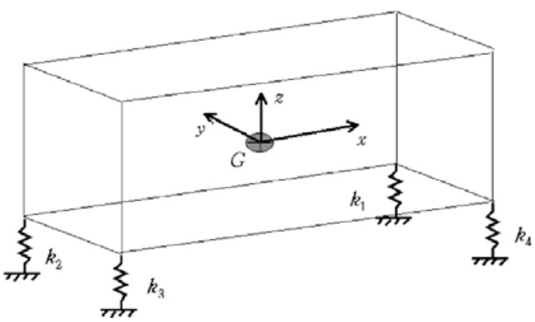

Fig. 9 Schematic diagram of an engine-mount system

Table 5 Positions of mounts with respect to the mass center of the engine

Mount No.	Coordinates [m]
k_1	(1.82, 0.55, −1.1)
k_2	(−1.82, 0.55, −1.1)
k_3	(−1.82, −0.55, −1.1)
k_4	(1.82, −0.55, −1.1)

The cost function minimizing the transmitted forces was chosen as the following Equation (22), which is different from Equation (20);

$$J=\sqrt{\sum_{i=1}^{4}(R_{x,i}^2+R_{y,i}^2+R_{z,i}^2)} \tag{22}$$

Here $R_{x,i}, R_{y,i}$, and $R_{z,i}$ denote the maximum values of the x, y, and z components of the forces transmitted through mount k_i. The other optimization processes are the same as those in Section 4.

Table 6 shows the optimized crank angles, which are different from both the initial values and the moment-minimized values. Fig. 11 shows the force transmitted through mount after the force optimization. The maximum forces before

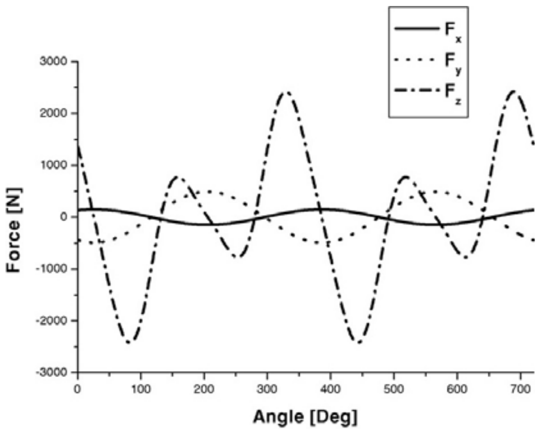

Fig. 10 Forces transmitted through mount k_1 with initial crank angles

Table 6 Initial and optimized crank angles minimizing the transmitted forces

Cylinder No.	Initial crank angle	Optimized crank angle
1	0.0°	0.0°
2	257.1°	257.4°
3	102.9°	104.7°
4	154.3°	156.6°
5	205.7°	210.1°
6	51.4°	56.1°
7	308.6°	314.1°

Table 7 Maximum forces transmitted through mounts

Components	Maximum forces [N]	
	Before optimized	After optimized
F_x	148.0	17.4
F_y	489.6	57.4
F_z	2421.3	1582.2

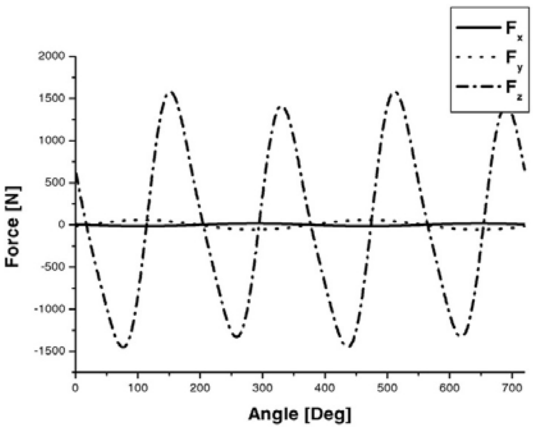

Fig. 11 Forces transmitted through mount k_1 with the optimized crank angles

and after the optimization are shown in Table 7. The reduction was 88% in the transverse direction and 35% in the longitudinal direction.

6. Conclusions

As described in this paper, the forces and moments exerted in an engine were formulated, and the results were verified by comparing the derived results with the manufacturer's specifications. After verifying the derived formula, a computer program was developed to optimize the exerted moments and transmitted forces. In the optimization process for crank angles in a seven-cylinder parallel engine, the crank angles were selected as design variables. The four equality constraint equations preserving the acting forces as zero were used to select two independent design variables.

Two kinds of optimization were carried out with the developed program in allocating crank angles to minimize moments or forces. After the optimization process, the evenly distributed crank angles were changed to uneven crank angles. With the optimized crank angles minimizing the exerting moments, the maximum reduction in a vertical moment was 72%, but the reduction of the guide moment was small because it came from the gas pressure in the cylinders. With the optimized crank angles minimizing the transmitted forces through the mounts, the reduction was 88% in the transverse components and 35% in the longitudinal components.

Although this study used only a marine engine, the optimization process could be applied to automobile engines in further research.

Acknowledgments

The authors would like to thank the Ministry of Science and Technology of Korea for its financial support through a grant (M1-0203-00-0017) under the NRL (National Research Laboratory) project.

References

Atkinson, K. E., 1978, "An Introduction to Numerical Analysis," John Wiley & Sons.

Cho, S. B., Ahn, S. H. and Yoo, H. S., 1995, "A Study on Optimization of Crankshaft in Diesel Engine," *Trans. of KSAE*, Vol. 3, No. 5, pp. 10∼16.

Connolly, F. T. and Yagle, A. E., 1994, "Modeling and Identification of the Combustion Pressure Process in Internal Combustion Engines," *Mechanical System and Signal Processing*, Vol. 8, No. 1, pp. 1∼19.

Denman, H. H., 1991, "Exact Solution for the Rigid Slider-Crank Mechanism with Gas Pressure," *Mechanism and Machine Theory*, Vol. 26, No. 4, pp. 415∼420.

Dubensky, R. G., 2002, "Crankshaft Concept Design Flowchart for Product Optimization," SAE 2002-01-0770, SAE International.

Haug, E. J. and Arora, J. S., 1979, "Applied Optimal Design," John Wiley & Sons.

Jacobsen, S. B. and Ronnedal, P., 1995, "Noise and Vibration Optimized 11-Cylinder Diesel Engine for Propulsion of 4800 TEU Container Vessel," *International Conference on Noise & Vibration in the Marine Environment*, 3 & 4, London, U.K.

Kang, D. K. and Yoo, W. S., 1995, "Effects of Hydro Engine Mount to the Vibration of Chassis," *Proceedings of the KSAE spring meeting*, pp. 386～391, Chungnam National University, Daejeon, Korea.

Kim, T. J., 2003, "Dynamic Analysis of a Reciprocating Compression Mechanism Considering Hydrodynamic Forces," *KSME Int. Journal*, Vol. 17, No. 6, pp. 843～853.

Paricha, M. S. and Carnegie, W. D., 1976, "Effects of Variable Inertia on the Damped Torsional Vibrations of Diesel Engine Systems," *J. of Sound and Vibration*, Vol. 46, No. 3, pp. 339～345.

Pasricha, M. S. and Carnegie, W. D., 1979, "Formulation of the Equations of Dynamic Motion Including the Effects of Variable Inertia on the Torsional Vibrations in Reciprocating Engines, Part I," *J. of Sound and Vibration*, Vol. 66, No. 2, pp. 181～186.

Ronnedal, P. and Nielsen, H. B., 2003, "Firing Order Selection in Relation to Vibration Aspects," ICES2003-603, 2003 Spring Technical Conference of the ASME Internal Combustion Engine Division, Salzburg, Austria, May 11-14.

Shangguan, W. B. and Lu, J. H., 2004, "Modeling of a Hydraulic Engine Mount with Fluid-Structure Interaction Finite Element An alysis," *J. of Sound and Vibration*, Vol. 275, No. 1-2, pp. 193～221.

Snyman, J. A., Heyns, P. S. and Vermeulen, P. J., 1955, "Vibration Isolation of a Mounted Engine Through Optimization," *Mechanism and Machine Theory*, Vol. 30, No. 1, pp. 109～118.

Suh, M. W., Shin, M. B., Kim, K. H. and Kim, K. H., 2003, "A Study on Efficient Generation of Beam-Mass Model for Simplification of the Crankshaft in the Large Marine Engine," *Trans. of KSME, Series A*, Vol. 27, No. 10, pp. 1661～1666.